Design of Type-III Controller for DC-DC Switch-Mode Boost Converter

Arnab Ghosh, *Student Member, IEEE*, and Subrata Banerjee, *Member, IEEE*

Department of Electrical Engineering, National Institute of Technology, Durgapur 713209, India.
E-mail: aghosh.ee@gmail.com, bansub2004@rediffmail.com

***Abstract*—DC-DC power converters have played a key role for different fields applications. Such demanding applications have been required a steady source of voltage irrespective any changes in line and load. The steady-state behaviors of these power-supplies have been defined by the converter topology. But the controller has taken place an important role for maintaining the accurate transient *i.e.* dynamic performance in dc-dc power-supplies. Some dc-dc power-supplies *like* boost, buck-boost *etc* have a *right-half-plane zero i.e.* there is a problem of *non-minimum phase*, so it is difficult for the PID controller to exhibit good performance. For this reason a special kind of classical controller *i.e. Type-III controller* is introduced for obtaining better performance. This paper describes the designing of a Type-III controller for a dc-dc switched-mode boost converter.**

Keywords—Switch-Mode-Power-Converter; Boost Converter; Non-Minimum Phase System; Type-III Controller Designing.

I. INTRODUCTION

The dc-dc power supplies have made remarkable place almost every sphere of engineering. The introduction of these power supplies has enhanced the technological and economical attributes with wide range of applications from a few tens of watts to several hundreds of megawatts. The most common and essential applications are such as personal/laptop computers, cellular phones, battery chargers, microprocessor kit, spacecraft, telecommunication system, high voltage dc transmission, adjustable motor drives and many others [1][2].

In the early days of dc power utilization, the potential dividers (PD's) were used to control and transfer the flow of dc power from one level to another level to the load. Though the construction and operation of the PD's are much simpler to realize but their uses have been decreased due to several limitations: (a) less energy efficient (because efficiency depends on the resistive values of the PD's), (b) difficult to step up the load voltage, (c) unregulated load voltage *etc*. For improving of energy efficiency, the linear regulators were introduced. The operations of linear regulators which are almost similar to the PD's embedded with load regulation features and the series resistance is replaced by solid state device. In linear regulators the solid state device operates in active zone incurring a significant amount of power losses across it. So, heat sink is required to dissipate the generated heat. Due to the presence of heat sinks, and line-frequency transformer the size and the weight of the power supply is bulky in nature and it is not suitable and economical for large power applications in terms of energy efficiency. But in Switch-Mode Power Supplies (SMPS) the solid state device works *like* a switch *i.e.* either completely *on* or *off*. Therefore, when the device is *on i.e.* conducting, large current flows through it with taking almost zero voltage across it. Similarly when the device is *off*, the voltage across the device is high with almost zero current through it. In both the cases the total power losses across the device is almost zero, so there are no conduction losses in switching regulators. So, energy efficiency is very high (extended up to 95%) in switching regulator and those are found wide applications in many fields engineering.

Over the last decades the technical developments of dc-dc switching converters are taken place by the introduction of different types of controller [8-16] for achieving fast dynamic response as well as better reliability and power density. The performance of dc-dc switching converter can be broadly classified into two categories: (a) transient performance, and (b) steady-state performance. The steady-state performance is mainly guided by the converter-topology, structural configuration of energy storage elements and operating frequency of the power supplies. On the other hand, the transient performance of converter is maintained by the control scheme *i.e.* nature of the controllers. There are several classical controllers *like* PI, PID controllers; have been developed over the years to ensure desired performance of the converter under specific conditions. Some converters *like* boost, buck-boost, and fly-back have a *right-half-plane zero* (*non minimum phase* system) [3], so it is difficult for the PID controller to exhibit good performance with load, line variations and parametric uncertainty. For this reason *Type-controllers* [4] are best suited. The *state-space averaging* [5-7] methods have been used for mathematical modelling of converter. The main objective of this paper is to design *Type-III controller* for a boost converter and check the converter's closed loop stability in time and frequency domain.

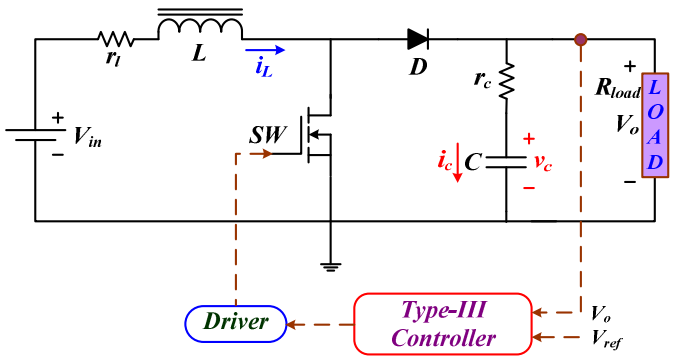

Figure 1: Power circuit diagram of a dc-dc boost converter.

978-1-4799-6042-2/14/$31.00 ©2014 IEEE

II. Converter Small Signal Model

A. Transfer Function of Boost Converter

The small signal [5-7] modeling of dc-dc switched-mode boost converter transfer function is written in equation (1).

$$T_p(s) = \frac{\tilde{v}_0(s)}{\tilde{d}(s)} = G_{do} \frac{\left(1+\frac{s}{\omega_{z-ESR}}\right)\left(1-\frac{s}{\omega_{z-RHP}}\right)}{\left\{1+\frac{s}{\omega_o Q}+\frac{s^2}{\omega_o^2}\right\}} \quad (1)$$

$where,\ G_{do} = V_{in}/(1-D)^2;\ \omega_{z-ESR} = 1/r_c C$ rad/sec;

$\omega_{z-RHP} = (1-D)^2 (R_{load} - r_l)/L$ rad/sec;

$\omega_o = \sqrt{\left[r_l + (1-D)^2 R_{load}\right]/LCR_{load}}$ rad/sec;

$$Q = \omega_o \Big/ \left(\frac{r_l}{L} + \frac{1}{C(R_{load}+r_c)}\right)$$

From the equation (1), it has been observed that a *right-half plane zero* presents in the transfer function of boost-converter. So, the effect of *non-minimum phase* problem has occurred in converter dynamics. That's why an initial undershoot is coming in Figure 2 and bode plot has shown the sufficient phase-lag at gain crossover frequency (Figure 3).

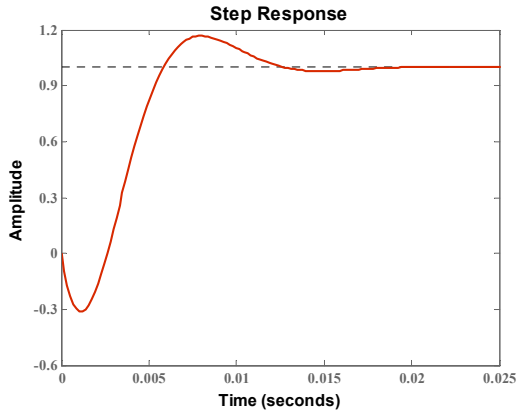

Figure 2: Time response of boost converter.

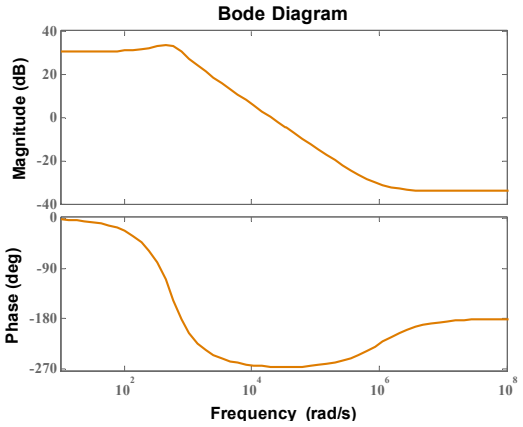

Figure 3: Frequency response of boost-converter.

TABLE I: Parameters of Boost Converter

Circuit Components	Values
Input Voltage V_{in}	5 Volt
Output Voltage V_o	12 Volt
Inductance L	250 µH
Output Capacitance C	1056 µF
Inductor Resistance r_l	10 mΩ
ESR of Capacitor r_c	30 mΩ
Load Resistance R_{load}	25 Ω
Switching Period T	50 μs

III. Type-III Controller Design

The design of controller plays a key role for maintaining good performance and regulation of a power supply. The controller which is the combination of poles-zeros provides the classical loop shape by modifying the gain and phase characteristics of open-loop frequency response as well as ensures the converter robustness. The "Type-III" controller is a lead-lead type controller with a pole at origin. So, this controller provides 0° to 180° *phase boost* with *zero steady state error*. Even though boost converter having non-minimum phase problem, it exhibits a better closed loop performance utilizing a cascaded Type-III controller. With proper tuning of the controller parameters, the fastest closed-loop performance can be achieved with minimal overshoots and zero steady-state error.

A. Mathematical Approach

Type-III controller is a pair of pole-zero combination with a pole at origin.

$$T_c(s) = \frac{(1+s/\omega_{z1})(1+s/\omega_{z2})}{(s/\omega_{po})(1+s/\omega_{p1})(1+s/\omega_{p2})} \quad (2)$$

Now the two zeros have been assumed at same point and similarly the two poles are also presumed same point so the location of *double pole* and *double zero* have been considered at $\omega_{z1} = \omega_{z2} = \omega_{z1,2}$ and $\omega_{p1} = \omega_{p2} = \omega_{p1,2}$.

$$T_c(s) = \frac{\left(1+\frac{s}{\omega_{z1,2}}\right)^2}{\left(\frac{s}{\omega_{po}}\right)\left(1+\frac{s}{\omega_{p1,2}}\right)^2} \quad (3)$$

The magnitude of the controller transfer function can be found by replacing s with $j\omega$ at equation (3).

$$\left|T_c(j\omega)\right| = \frac{\left|1+j\frac{\omega}{\omega_{z1,2}}\right|\left|1+j\frac{\omega}{\omega_{z1,2}}\right|}{\left|j\frac{\omega}{\omega_{po}}\right|\left|1+j\frac{\omega}{\omega_{p1,2}}\right|\left|1+j\frac{\omega}{\omega_{p1,2}}\right|}$$

$$or,\ \left|T_c(j\omega)\right| = \frac{\left(1+\left(\frac{\omega}{\omega_{z1,2}}\right)^2\right)}{\left(\frac{\omega}{\omega_{po}}\right)\left(1+\left(\frac{\omega}{\omega_{p1,2}}\right)^2\right)} \tag{4}$$

The argument can be written as

$$\arg T_c(j\omega) = 2\tan^{-1}\left(\frac{\omega}{\omega_{z1,2}}\right) - 2\tan^{-1}\left(\frac{\omega}{\omega_{p1,2}}\right) - \frac{\pi}{2} \tag{5}$$

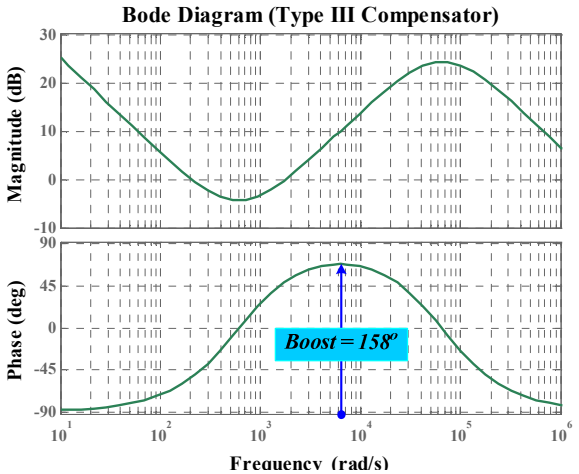

Figure 4: The Bode diagram of Type-III controller.

The frequency domain response of Type-III controller has been plotted in Figure 4. Here the pole-zero combinations create a local phase boosting of 158° at a certain frequency. If locations of both poles and zeros have been varied the phase lead also is to be changed. In case of Type-III controller the maximum 180° phase boost may be obtained.

The *frequency* where the *maximum phase boost* will be occurred can easily obtain by derivate equation (5)

$$\frac{d}{df}\left(\arg T_c(j\omega)\right) = \frac{d}{df}\left(2\tan^{-1}\left(\frac{f}{f_{z1,2}}\right) - 2\tan^{-1}\left(\frac{f}{f_{p1,2}}\right)\right)$$

$$or, \qquad = \frac{2}{f_z\left(\frac{f^2}{f_{z1,2}^2}+1\right)} - \frac{2}{f_p\left(\frac{f^2}{f_{p1,2}^2}+1\right)} = 0 \tag{6}$$

By solving f, from the equation (6), the *maximum phase boost* can be obtained at the *geometric means* of the double zero-double pole frequencies:

$$f_{\max} = \sqrt{f_{z1,2}f_{p1,2}} \tag{7}$$

Generally this geometric mean frequency is considered as crossover frequency (f_c) of the controller.

B. *Derivation of k in Type-III Controller*

The k is defined as the ratio of the double pole frequency to the double zero frequency in Type-III controller. These poles-zeros combination provide maximum boost 180° at the cross over frequency. So it has been needed to equate the relation between k and the *phase boost* of the controller.

Initially both terms are unknown, so there must be two equations:

$$phase\ boost = 2\left(\tan^{-1}\left(\frac{f_c}{f_{z1,2}}\right) - \tan^{-1}\left(\frac{f_c}{f_{p1,2}}\right)\right) \tag{8}$$

$$\text{and}\ \ f_c = f_{\max} = \sqrt{f_{z1,2}f_{p1,2}} \tag{9}$$

$$\text{So,}\ \ f_{z1,2} = \frac{f_c^2}{f_{p1,2}} \tag{10}$$

Now $f_{z1,2}$ is substituted in (8)

$$phase\ boost = 2\left(\tan^{-1}\left(\frac{f_{p1,2}}{f_c}\right) - \tan^{-1}\left(\frac{f_c}{f_{p1,2}}\right)\right) \tag{11}$$

To solve this equation, k has been introduced

$$\text{where}\quad k = f_{p1,2}^2 \big/ f_{z1,2}^2 \tag{12}$$

$$\text{So,}\ \ phase\ boost = 2\left(\tan^{-1}\left(\sqrt{k}\right) - \tan^{-1}\left(\frac{1}{\sqrt{k}}\right)\right) \tag{13}$$

From the trigonometric formula

$$2\left(\tan^{-1}\left(\sqrt{k}\right) + \tan^{-1}\left(\frac{1}{\sqrt{k}}\right)\right) = \pi \tag{14}$$

From (13) and (14)

$$4\tan^{-1}\left(\sqrt{k}\right) = phase\ boost + \pi \tag{15}$$

By solving k from (15)

$$k = \left\{\tan\left(\frac{phase\ boost}{4} + \frac{\pi}{4}\right)\right\}^2 \tag{16}$$

This expression is known as "*k factor*" approach, was introduced by Dean Venable [4].

So the pole location will be (from (12))

$$f_{p1,2} = \sqrt{k}.f_c = \tan\left(\frac{phase\ boost}{4} + \frac{\pi}{4}\right)f_c \tag{17}$$

and the zero is derived from:

$$f_{z1,2} = \frac{f_c}{\sqrt{k}} = \frac{f_c}{\tan\left(\frac{phase\ boost}{4} + \frac{\pi}{4}\right)} \tag{18}$$

When the crossover frequency is known with the values of necessary phase boost, the exact locations of the double-pole/double-zero can be easily found from (17) and (18).

C. Mid-Band Gain Adjustment for the Controller

A Type-III controller is simply combination of *double pole/zero pair* with *an origin pole*. Controller has been described from equation (2)

$$T_c(s) = G_o \frac{(\omega_{z1}/s+1)(1+s/\omega_{z2})}{(1+s/\omega_{p1})(1+s/\omega_{p2})} \tag{19}$$

In the above expression, the term G_o is called the *mid-band gain* and G_o is equal to ω_{po}/ω_{z1}. The location of ω_{z1} should be fixed by the amount of needed phase boost and the location of ω_{po} is depending up on the required gain at crossover.

$$\text{Now, } G_o = G\frac{\sqrt{1+\left(\frac{\omega_c}{\omega_{p1}}\right)^2}\sqrt{1+\left(\frac{\omega_c}{\omega_{p2}}\right)^2}}{\sqrt{1+\left(\frac{\omega_{z1}}{\omega_c}\right)^2}\sqrt{1+\left(\frac{\omega_c}{\omega_{z2}}\right)^2}} \tag{20}$$

G is an *assumed gain* at crossover frequency f_c.

$$\text{So, } \omega_{po} = G.\omega_{z1}\frac{\sqrt{1+\left(\frac{\omega_c}{\omega_{p1}}\right)^2}\sqrt{1+\left(\frac{\omega_c}{\omega_{p2}}\right)^2}}{\sqrt{1+\left(\frac{\omega_{z1}}{\omega_c}\right)^2}\sqrt{1+\left(\frac{\omega_c}{\omega_{z2}}\right)^2}} \tag{21}$$

If double coincident poles/zeros pair has been considered, the formula becomes

$$\omega_{po} = G.\omega_{z1}\frac{\left(\omega_{p1,2}^2+\omega_c^2\right)}{\omega_{p1,2}^2\sqrt{\left(\frac{\omega_{z1,2}}{\omega_c}\right)^2+1}\sqrt{\left(\frac{\omega_c}{\omega_{z1,2}}\right)^2+1}} \tag{22}$$

IV. Design Example with a Type-III

Let's assume a power supply that has a gain deficit of -10 dB at a 1 kHz selected crossover frequency. The necessary phase boost is 158°. From equation (17) and (18), the position of the double pole is

$$f_{p1,2} = \tan\left(\frac{158^o}{4}+45^o\right)\times 1000 = 10.38 \text{ kHz} \tag{23}$$

and the double zero is placed at

$$f_{z1,2} = \frac{1000}{\tan\left(\frac{158^o}{4}+45^o\right)} = 96.28 \text{ Hz} \tag{24}$$

The gain G at 1 kHz must be -10 dB. So the position of the 0-dB crossover pole can be found from equation (22).

$$\text{So, } f_{po} = \frac{10^{\frac{-10}{-20}}\times 96.28\times 1000^2(10.38+1)}{10.38\times 1000^2\times\sqrt{1+\left(\frac{96.28}{1000}\right)^2}\sqrt{1+\left(\frac{1000}{96.28}\right)^2}} \tag{25}$$

$$= 29.30 \text{ Hz}$$

So the transfer function of the designed Type-III controller is given by $\frac{3.003' 10^6(s+605)^2}{s(s^2+1.31' 10^5 s+4.26' 10^9)}$.

V. Stability Analysis

A. Closed-loop performances: Adjustment of Controller Crossover Frequency (f_c)

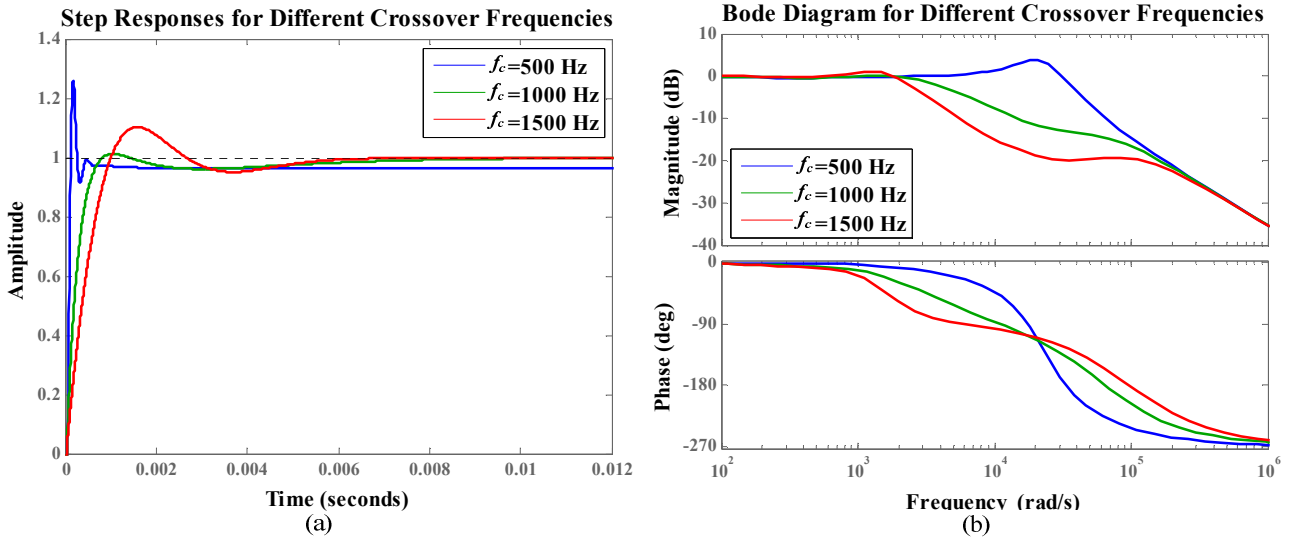

Figure 5: (a) Step responses (b) Bode Diagram of closed loop boost converter for different values of crossover frequency at constant controller gain 3.003×106.

The closed-loop performances of a dc-dc boost converter cascaded with Type-III controller has been studied with different cross over frequencies (f_c) for a constant gain (G_o). Since crossover frequency directly influences the pole, zero location of compensator, it has to be judiciously selected to get optimum performance. From Figure 5 (a) and (b) it is clear that for f_c=1 kHz, both the time and frequency responses are better than f_c=500 Hz and f_c=1.5 kHz. It is understood that if the f_c is increased beyond certain value than the performance of the closed loop converter deteriorates. Again for a lower value of f_c=500 Hz, the time response plot is not impressive and it exhibits more overshoots before reaching final steady-state point. The respective comparative performance details are also reported in TABLE II.

TABLE II: COMPARITIVE STUDY OF CLOSED-LOOP PERFORMANCES

Crossover Frequency (f_c)	500 Hz	1000 Hz	1500 Hz
Maximum Overshoot (M_p)	25.7 %	1.14 %	10.2 %
Rise time (t_r)	0.00012 sec	0.00080 sec	0.00101 sec
Phase margin (PM)	42.7°	78°	64.3°
Gain crossover frequency (GCF)	14600 rad/sec	3700 rad/sec	1980 rad/sec
Gain margin (GM)	6.47 dB	16 dB	20.4 dB
Phase Crossover Frequency (PCF)	32800 rad/sec	64900 rad/sec	96900 rad/sec
Controller Gain (G_o)	3.003×10^6	3.003×10^6	3.003×10^6
Controller Transfer Function (T_c)	$\frac{3.003'\ 10^6(s+303)^2}{s(s^2+6.53'\ 10^4 s+1.06'\ 10^9)}$	$\frac{3.003'\ 10^6(s+605)^2}{s(s^2+1.31'\ 10^5 s+4.26'\ 10^9)}$	$\frac{3.003'\ 10^6(s+907.5)^2}{s(s+97880)^2}$
Closed-Loop Stability	Stable	Stable	Stable

B. Closed-loop performance: Adjustment of Controller Gain

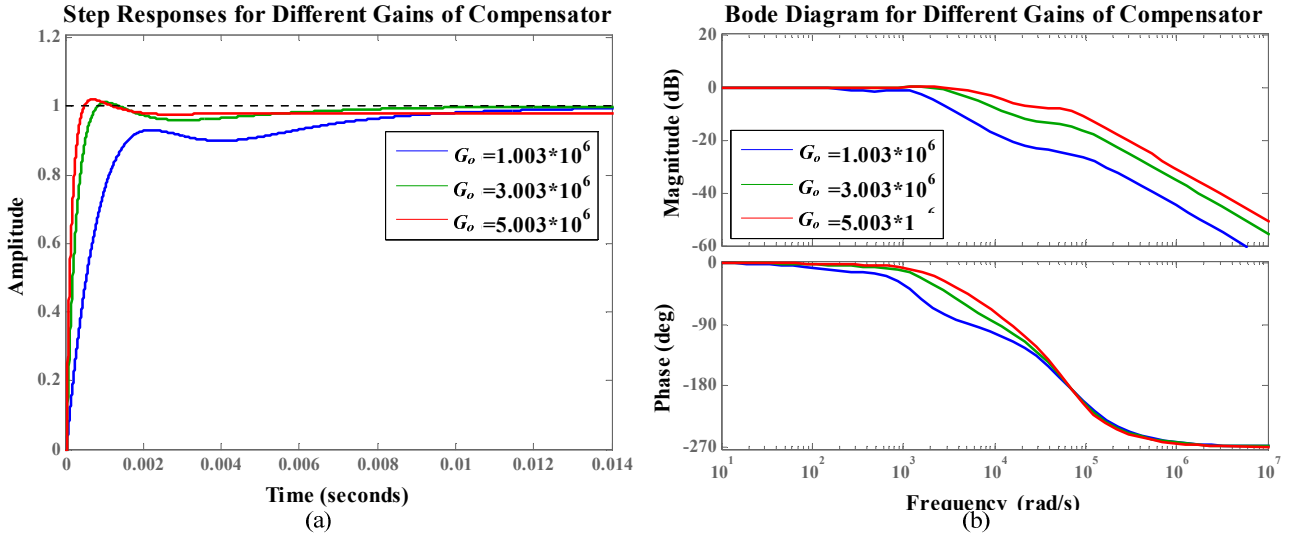

(a) (b)

Figure 6: (a) Step responses (b) Bode Diagram of closed loop boost converter with Type-III controller for different gains at constant crossover frequency 1 kHz.

The closed-loop performances of a boost converter have been shown in Figure 6 (a) and (b) with different values of controller gain G_o for a fixed crossover frequency of 1 kHz. Here the controller gain (G_o) has been increased from 1.003×10^6 to 5.003×10^6. Increasing the gain means the rise time will be reduced and consequently the peak overshoot will be increased. The comparative performance analyses are reported in TABLE III. It can be observed that the best response is found at gain (G_o) 3.003×10^6 for crossover frequency (f_c) of 1 kHz.

TABLE-III : COMPARITIVE STUDY OF CLOSED-LOOP PERFORMANCES

Controller Gain (G_o)	1.003×10^6	3.003×10^6	5.003×10^6
Crossover Frequency (f_c)	1 kHz	1 kHz	1 kHz
Maximum Overshoot (M_p)	0 %	1.14 %	1.98%
Rise time (t_r)	0.0150 sec	0.0008 sec	0.0005 sec
Phase margin(PM)	79.5°	78°	75.7°
Gain crossover frequency (GCF)	1470 rad/sec	3700 rad/sec	6150 rad/sec
Gain margin (GM)	25.5 dB	16 dB	11.6 dB
Phase Crossover Frequency (PCF)	64900 rad/sec	64900 rad/sec	64900 rad/sec
Controller Transfer Function (T_c)	$\frac{1.003' 10^6 (s+605)^2}{s\left(s^2+1.31' 10^5 s+4.26' 10^9\right)}$	$\frac{3.003' 10^6 (s+605)^2}{s\left(s^2+1.31' 10^5 s+4.26' 10^9\right)}$	$\frac{5.003' 10^6 (s+605)^2}{s\left(s^2+1.31' 10^5 s+4.26' 10^9\right)}$
Closed-Loop Stability	Stable	Stable	Stable

VI. CONCLUSION

This work describes design of a Type-III controller for a dc-dc switch-mode boost converter. The cascade compensated closed-loop converter has been simulated. The effect of crossover frequency (f_c) and gain (G_o) on the *closed loop stability & performance* of the boost converter has been investigated. These two parameters finally decide the controller transfer function. The closed loop behavior of power supply with Type-III controller is satisfactory. But for obtaining better results the parameters of controller have to be optimized by soft-computing techniques and this may be a part of future work.

REFERENCES

[1] N. Mohan, T. M. Undeland, and W. P. Robbins, "Power Electronics," 3rd ed. New York: Wiley, 2003.

[2] M. H Rashid, "Power Electronics – Devices, Circuits and Applications," Pearson Publishing, 2014.

[3] K. Ogata, "Modern Control Engineering," 5th ed. Pearson Education, India, 2010.

[4] H. Dean Venable, "The k-factor: A New Mathematical Tool for Stability Analysis and Synthesis," Proceedings of Powercon 10, CA, March 22-24, 1983.

[5] R. D. Middlebrook, and S. Cuk, "A General Unified Approach To Modelling Switching-Converter Power Stages," Proceedings of the IEEE Pwer Electr~nics Specialists Conference, June 1976.

[6] R. D. Middlebrook, "Small-Signal Modeling of Pulse-Width modulated Switched-Mode Power Converters," Proceedings of The IEEE, Vol. 76, No. 4, April 1988.

[7] Y. S. Lee, "Computer-Aided Analysis and Design of Switch-Mode Power Supplies," Marcel Dekker, Inc. Hong Kong. 1993.

[8] C. M. Liaw, S. J. Chiang, C.Y. Lai, K.H. Pan, G.C. Leu, and G. S. Hsu, "Modeling and Controller Design of a urrent-Mode Controlled Converter,"IEEE Transacttons On Industrial Electronics, Vol. 41, No.2, April 1994.

[9] J. H. Su, J. J. Chen, and D.S. Wu, "Learning Feedback Controller Design of Switching Converters Via MATLAB/SIMULINK," IEEE Transactions On Education, Vol. 45, No. 4, November 2002.

[10] B. Bryant, and M. K. Kazimierczuk, "Modeling the Closed-Current Loop of PWM Boost DC–DC Converters Operating in CCM With Peak Current-Mode Control," IEEE Transactions On Circuits And Systems—I: Regular Papers, Vol. 52, No. 11, November 2005.

[11] T. Geyer, G. Papafotiou, and M. Morari, "Hybrid Model Predictive Control of the Step-Down DC-DC Converter," IEEE Transactions On Control Systems Technology, Vol. 16, No. 6, November 2008.

[12] K. I. Hwu, and Y. T. Yau, "Performance Enhancement of Boost Converter Based on PID Controller Plus Linear-to-Nonlinear Translator," IEEE Transactions On Power Electronics, Vol. 25, No. 5, May 2010.

[13] J-K. Kuo and C-F. Wang, "An integrated simulation model for PEM fuel cell power systems with a buck DC-DC converter," International Journal of Hydrogen Energy, vol. 36, pp. 11846-11855, 2011.

[14] A. Ghosh, "Nonlinear Dynamics of Power-Factor-Corrected AC-DC Boost Regulator: Power Converter, Nonlinear Phenomena, Controlling The Nonlinearity," LAP Lambert Academic Publishing, 2012.

[15] A. Ghosh, S. Banerjee, P.K. Saha, and G.K. Panda, "Nonlinear Modeling and Bifurcations in Switched Power-Factor-Correction Boost Regulator" in IEEE International Conference on Circuits, Power and Computing Technologies (ICCPCT), pp. 517-522, 2013. (IEEE *Xplore* D.O.I. Publication 10.1109/ICCPCT.2013.6528938).

[16] P. Karamanakos, T. Geyer, and S. Manias, "Direct Voltage Control of DC-DC Boost Converters Using Enumeration-Based Model Predictive Control," IEEE Transactions On Power Electronics, Vol. 29, No. 2, February 2014.